Debris studies for the tin-based droplet laser-plasma EUV source

K. Takenoshita, C-S. Koay, S. Teerawattanasook, M. Richardson
Laser Plasma Laboratory, School of Optics-CREOL at University of Central Florida

ABSTRACT

We are developing a mass-limited, laser plasma target concept that utilizes excited state transitions in tin ions as the source of 13.5 nm radiation, offering in-band conversion efficiencies greater than 1%. The ultimate objective of this EUV source strategy is the utilization of a target that is completely ionized by the laser. To determine the viability of this source for EUVL, we are making extensive measurements of the debris emanating from the target. Here we report on some of these measurements.
Also under investigation are various methods of debris mitigation. We have previously shown the effectiveness of electrostatic fields for repelling ions from mass-limited targets, demonstrating improvements in multilayer mirror lifetimes in excess of an order of magnitude, positioning water droplet targets within reach of the EUVL roadmap requirements. Our investigation of debris utilizes various diagnostic techniques including ion collection, ion sputtering and witness-plate capture of particulate debris, and extensive post-mortem microscopic materials analysis.

Keywords: EUV source, tin plasma, debris, ion spectra, inhibition, mitigation.

1. INTRODUCTION

Light source development is one of the key elements in the progress of EUV lithography as it moves towards becoming the technology for fabrication of the next generation microchips. The EUV source is required to radiate adequate light at 13.5 nm, compatible with the narrowband Mo-Si multilayer mirrors used in the collection and imaging optics which transfer the EUV light energy to the wafer. There are two approaches to generating the required EUV radiation in a compact footprint, Laser Produced Plasmas (LPP) and Gas Discharge Produced Plasmas (GDPP). Both sources face two critical issues: meeting sufficient EUV light conversion efficiency and minimizing the emission of particulate debris. Until now both approaches have mainly investigated Xe as the source material, with the belief that gas will provide negligible debris emission. Due to the low conversion efficiency of Xe at 13.5nm, extremely high-power lasers or high-energy discharge circuits will be necessary to supply sufficient EUV at the intermediate focus where the EUV light source specification is determined[1]. In 2001, our laboratory began investigating mass-limited laser plasma sources containing tin as an alternate source material[2], and since then significant improvements in the conversion efficiency have been reported, particularly in 2003[3-5]. This change to tin as a source material makes EUVL systems more realizable but consequently, makes the debris issue more important and more critical than before.

The debris issue has to be addressed in different ways for LPP and GDPP sources due to the differences in the type of debris and in the light collection methods used. For the LPP EUV sources, the large collection angle, typically 2π sr, and its plasma size, typically much smaller than 1mm, are advantageous over GDPP sources. Normal incident Mo-Si multilayer mirrors, a so-called 'condenser mirror' or C1 mirror, are used to collect the EUV emission over 2π. The lifetime of the EUV source system is determined by how long the condenser mirror reflectivity remains within 10% of its maximum value. Since the mirrors are located in line-of-sight to the plasma source, all the radiation from the source (regardless of wavelength), high velocity ions, neutral atoms, ejected electrons from the target, clusters of target material, and particulate matter in liquid or solid state can damage the mirrors.

We have been investigating several types of target materials and geometries for suitable EUV sources since 1992[6-8]. This extensive background in source development has led to an ideal target concept, the so called mass-limited target. A mass-limited target is one in which its mass is just sufficient for the target to be completely ionized during its interaction with a laser pulse. It is expected that the first condenser mirror's lifetime is significantly increased by using the mass-

Emerging Lithographic Technologies VIII, edited by R. Scott Mackay,
Proceedings of SPIE Vol. 5374 (SPIE, Bellingham, WA, 2004)
0277-786X/04/$15 · doi: 10.1117/12.541533

limited target. We have also realized a mass-limited target containing tin with high conversion efficiencies previously reported[2]. In addition, we previously reported the first results of the impact of debris on the multilayer mirror optics with these targets[9]. A number of small particles deposited on the mirror surface were observed. The deposited particles were characterized in their spatial distribution, their sizes, and profiles were characterized by Optical Microscopy (OM), Scanning Electron Microscopy (SEM), Auger Electron Microscopy (AEM) and Atomic Force Microscopy (AFM). The aforementioned particles deposited on the mirror surface were identified as tin by X-ray Photoelectron Spectroscopy (XPS) and Auger Electron Spectroscopy (AES). To maintain the reflectivity of the condenser mirror, it is necessary to reduce or eliminate any particulate or ion emission from the plasma which will result in degradation of the mirror reflectivity, especially these particles.

Degradation of the condenser mirror reflectivity can be caused by different mechanisms. Fast ions or neutral atoms produced by the laser-material interaction can cause erosion of the mirror material. We have observed that oxygen ions ablate the multilayer mirror material over a number of laser shots[10]. Neutral atoms or slow ions from the target material can chemically interact with mirror elements. For instance, we have observed that oxidation of the mirror surface results from oxygen ions that were slowed down by a buffer gas[10]. At high speeds clusters of target material can chip off the mirror surface or at low speeds they can deposit on the surface.

Debris inhibition is necessary to prevent all these degradation mechanisms. A number of techniques have been investigated such as the use of electric fields, buffer gases, and a secondary plasma[11-13]. By utilizing an electrostatic field inhibition technique, the repeller field has demonstrated mirror reflectivity lifetime improvement by at least one order of magnitude when used with laser plasma water target sources[10]. At that time, the kinetic energy of those ions was not measured. Similarly, an explanation was not made concerning how those ions were repelled by the field. It is important to measure the ion velocity for a better understanding the laser material interaction. For example, if through ion measurements we observed that more of the target material is ionized, then we can presume that less particulate matter is generated. Consequently, we can then draw the conclusion that degradation of mirror reflectivity occurs predominantly due to ionic debris.

Here we report studies 1) to measure ions energies so that we can estimate how these ions affect the mirror surface, and 2) to investigate the effectiveness of the repeller field for ions and particulate matter.

2. EXPERIMENTAL SETUP

Our dedicated facility for debris studies consists of a target chamber, laser system, a target dispenser, and debris diagnostics. The target chamber provides all necessary port accesses of laser-material interaction and diagnostics and is kept at a vacuum pressure of approximately 4×10^{-4} Torr. A commercial high repetition rate Q-switched Nd:YAG laser (Spectra-Physics Quanta-ray GCR-190) is used for creating the laser plasma from our mass-limited targets. The average laser pulse energy is 340mJ, pulse duration ~10ns, and repetition rate 100Hz. The laser beam is focused onto the target using a lens with focal length of 50mm, which gives intensities of approximately 6.8×10^{11}W/cm^2 at the focal spot whose diameter is 70μm.

The target dispenser produces a train of droplets of uniform size that is adjustable by applying different driving frequencies to a piezo-crystal attached to the capillary nozzle. The typical target diameter is about 30~40μm. Tin is doped into a water solution at a concentration of about 30% by mass. Unused targets are captured by a cryogenic cold trap in order to prevent evaporation in the vacuum chamber, which will otherwise result in an increase in pressure.

The debris diagnostics are configured orthogonal to the incident laser direction. Detailed descriptions are provided in the following two sections. A picture of the experimental setup is shown in Fig. 1.

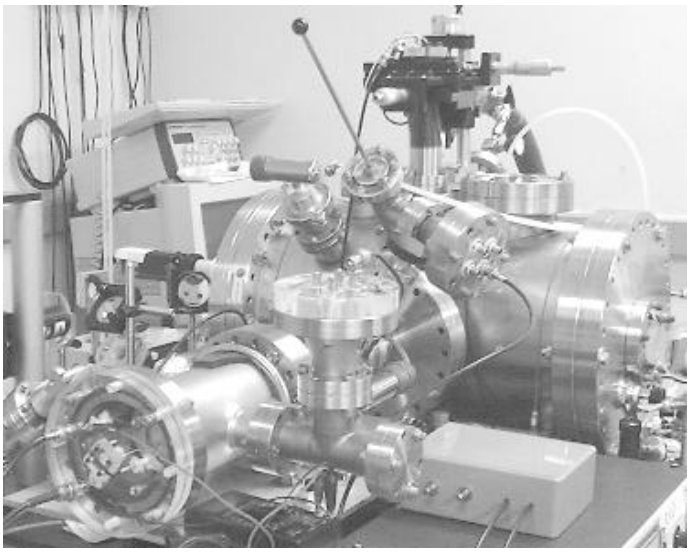

Figure 1: Experimental Setup

2.1. Ion measurement

Two different approaches are used to measure ionic debris. The first is a Faraday Cup Ion Probe (IP) and the second a custom designed Ion Spectrometer configured as an Ion Energy Analyzer (IEA). The IP and IEA configurations are shown in Fig. 2. Both of them utilize Time of flight (TOF) analysis and are both commonly used in many fields[14-16].

The IP collects various charged particles unless an electrostatic potential is applied to the grid located in front of the cup's electrode. To measure positively charged ions, a negative potential is applied which is typically -60V. At the beginning of the laser-material interaction, the IP experiences strong X-ray radiation from the source generating photoelectrons on the cup electrode. This photoelectron signal determines the plasma event time used for the TOF measurements. The charge signal is detected when individual charged particles arrive at the cup's electrode. From the time-delay, the time of flight, and the distance between IP and the source, the velocity of the particle can be determined by assuming the particles fly at constant velocity. From this, and by using the mass of ion, the particle's kinetic energy can be calculated.

While IP collects a variety of particles, the ion spectrometer detects selected ions with a corresponding kinetic energy. Under the influence of the electrostatic force, the ions that fail to get through the IEA's geometric path are filtered out. The trajectory path is a circular quadrant illustrated in Fig. 2. The IEA passes only those ions with specific kinetic energy of product of Z and E. With the same kinetic energy, the velocity varies for different elements due to their different mass. Thus the IEA first analyzes ions of higher Z and smaller mass processing down through to the lowest Z and the heaviest ion. These analyzed ions hit the electron multiplier surface and generate secondary electrons that are then multiplied to generate detectable signals. To use the electron multiplier properly, the vacuum of entire ion spectrometer assembly must be kept less than $1.0X10^{-5}$Torr.

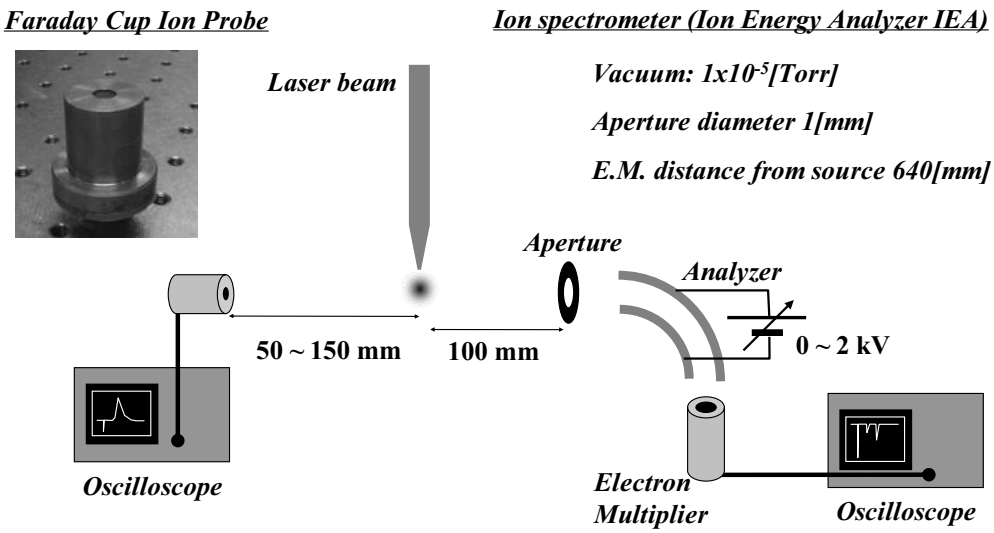

Figure 2: Two methods of ion measurement

2.2. Particulate debris detection and mitigation

Particulate debris detection is performed using post shot analysis. The detection and mitigation setup is shown in Fig. 3. Witness plates consisting of pieces of silicon wafer are placed at a distance of 64mm from the source. For debris inhibition, the repeller field is installed in front of the plates. A stainless steal mesh of 70% optical transmission is used as the field electrode. In order that witness plates capture debris only from the stable laser-target interaction, a slow shutter is installed in front of the inhibition structure. The shutter is opened when the laser-target interaction is stabilized, and is closed after a specific number of shots. A grounded collimator is installed in front of the witness plate so that the area exposed to the plasma can be distinguished from an unexposed area. The experimental apparatus is designed in such a manner as to allow the removal and installation of witness plates during an experiment. The experiments are carried out with a laser pulse energy of 340mJ, and the number of shots for each exposure is $3x10^4$.

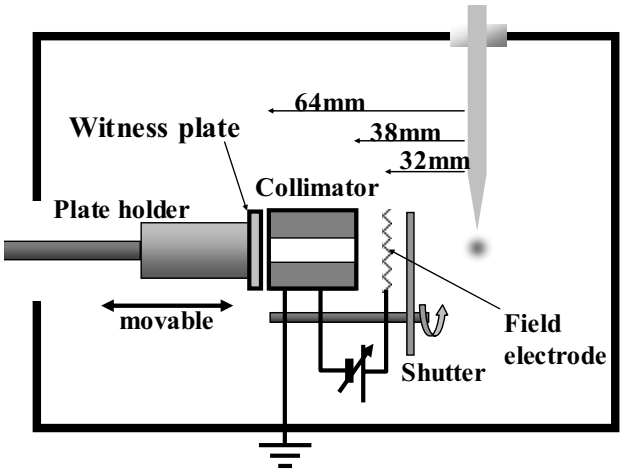

Figure 3: Experimental setup for debris detection and repeller field inhibition

3. RESULTS

3.1. Ion measurement for laser plasma from tin doped target

3.1.1. Measurement with ion probe

Ion signals measured by the ion probe are shown in Fig. 4. Signals are measured at various distances. For the purpose of comparison, the TOF of all the signals shown are rescaled to an equivalent distance (150mm) .Using the TOF corresponding to the location at the peak signal, the ion velocity can be estimated. Ion velocity estimations for three types of plasma sources are: $1.2x10^5$m/s for water droplet target, $1.1x10^5$m/s for Tin 20% doped target and $1.0x10^5$m/s for tin 30% doped target. It is observed that ion velocities are lower for higher concentration tin-doped targets.

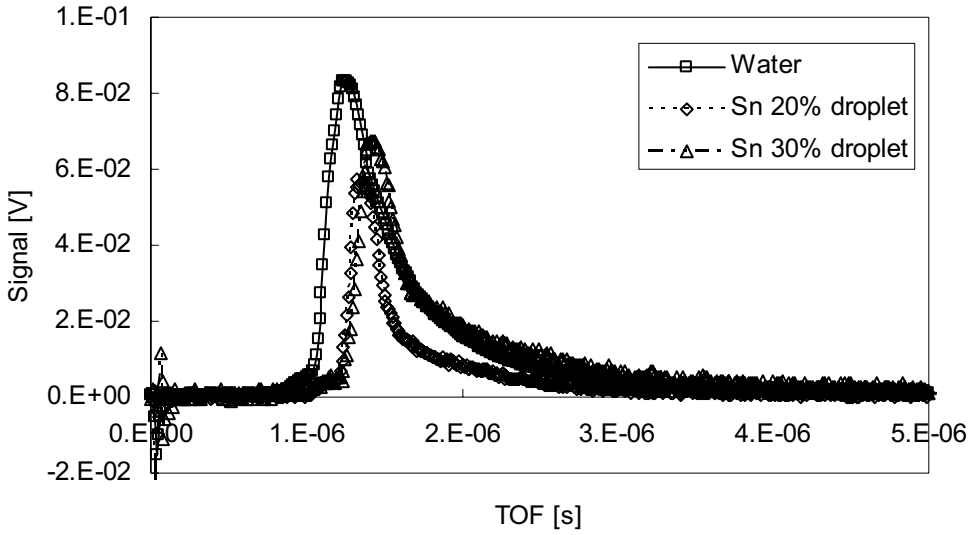

Figure 4: Ion probe signals from the water droplet target and tin doped droplet targets.

A separate ion measurement was performed in the case of the solid tin planar target to compare the ion velocity from a 100% tin concentration target to the velocities of ions from water droplet targets and Tin-doped droplet targets. Figure 5 shows the ion signal from the solid tin planar target. The signal is measured 150mm from the target so that it can be easily compared to the signals from the water and tin-doped droplet targets. The velocity of the peak is calculated to be $5.8x10^4$m/s which is less than a half of the velocity from water droplet targets. This series of ion signals indicate that doping of tin causes ion signals to slow down, which is to be expected, because the mass of a tin atom is significantly larger than the mass of hydrogen and oxygen ions for the same kinetic energy. To confirm this trend, the ion spectrometer is used to decompose the ion species making up the ion probe signal.

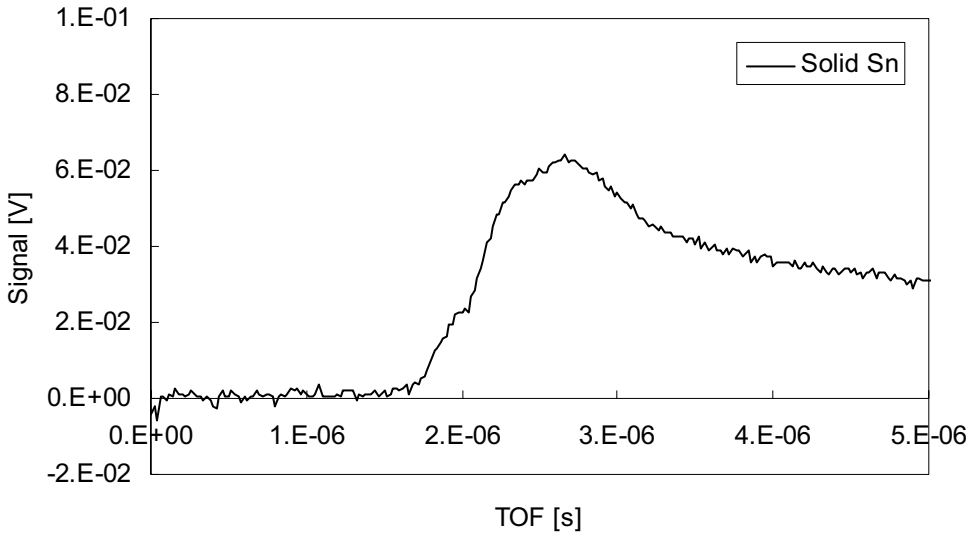

Figure 5: Ion probe signal from solid tin planer target

3.1.2. Measurement with ion spectrometer

Typical ion spectra are shown Fig. 6. The signal from the water target is shown for (a) one whose product of analyzed ion kinetic energy E and charge state Z is 250eV, and the signal from tin 30% doped target is shown for (b) one whose product of E and Z is 313eV. In both signals, the ion probe signals are also shown as references when converted to the same distance of the electron multiplier in the ion spectrometer.

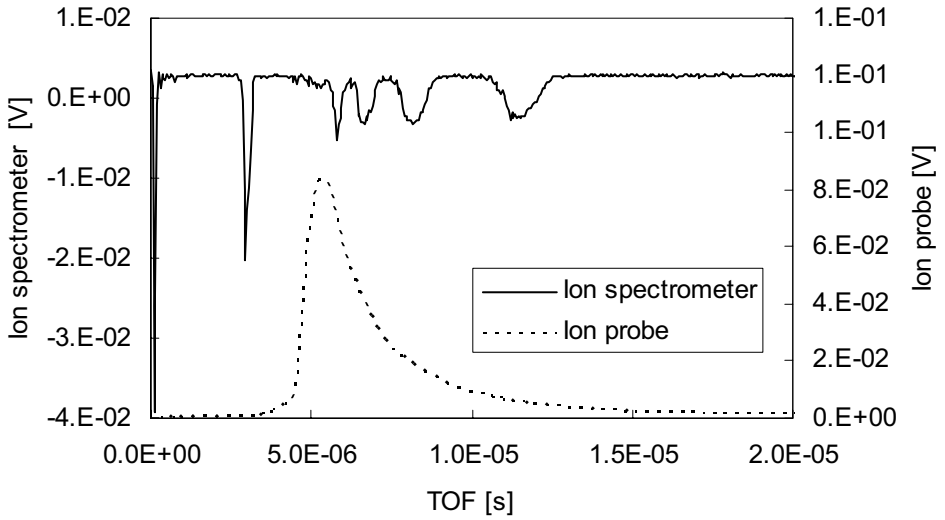

Figure 6: (a) Ion spectrum and ion probe signal from water droplet target

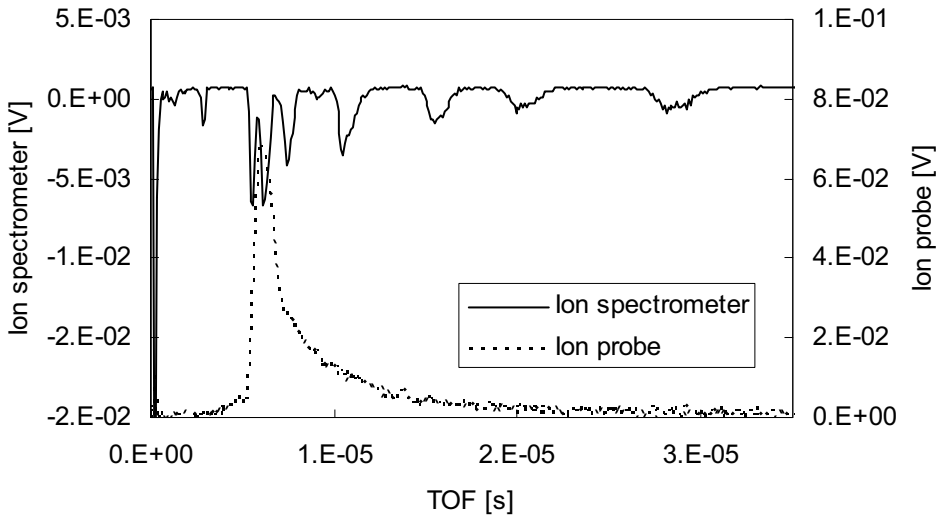

Figure 6: (b) Ion spectrum and ion probe signal from Tin 30% doped droplet target.

Signals from different ion species are observed from both types of target. One peak in the ion spectrometer signal is observed before the peak of the ion probe signal and is evident for both targets. Also, at least four lines around the peak and the decaying region in the ion probe signal are observed. The first signal is most likely from hydrogen and the latter signals are from oxygen (in Fig 6 (a)). As expected, four more signals are detected after the later part of the decay of the ion probe signal from a tin doped target. These signals agreed well to the calculation of TOF based on the analyzed kinetic energy. For instance, a hydrogen ion with 250eV has a velocity of 2.2×10^5m/s which reaches the electron multiplier in 2.9μs traveling a distance of 0.64m from the target. Similarly, each ion spectrum can be identified as a specific ion. More detailed investigations in different analyzed energies in combination with more advanced measurement methods such as a Thomson parabola are in progress.

3.2. Inhibition for particulate debris and ions

3.2.1. Effect of repeller field for particulate debris

Since particulate matter was found on the multilayer mirror surfaces[9] that are exposed by locating them facing towards the plasma created from a tin-doped target, it is very important to inhibit these particle depositions to maintain the mirror reflectivity. Our previous results showed that the repeller field succeeded in stopping a fraction of these particles[9]. Our new setup allows us to investigate more precisely and more consistently the effectiveness of the field inhibition scheme by comparing two witness plates placed in one experiment: one without the field applied, and the other with the field applied. Figure 7 shows the images of the two witness plates (Si wafer) with surfaces area of 50μm x 50μm, after 3×10^4 laser shots, and distance from the source of 64mm. Figs (a) and (b) are Auger Electron Microscopy images and (c) and (d) are the elemental mapping of the tin signal of the same areas of (a) and (b) respectively. Significantly less tin particle depositions are observed on the surface with the repeller field than without it. This is an important conclusion, since it indicates that the repeller field can mitigate against particulate debris as well as ions.

The tin deposition, however, is not completely inhibited. The potential of the field electrode is 640V which is the maximum voltage that did not create a discharge between the electrode and grounded components in the configuration. There are possibilities to improve the effectiveness of the inhibition by changing the configuration such that far less deposition is observed. It may also be important to combine other inhibition methods with the repeller field.

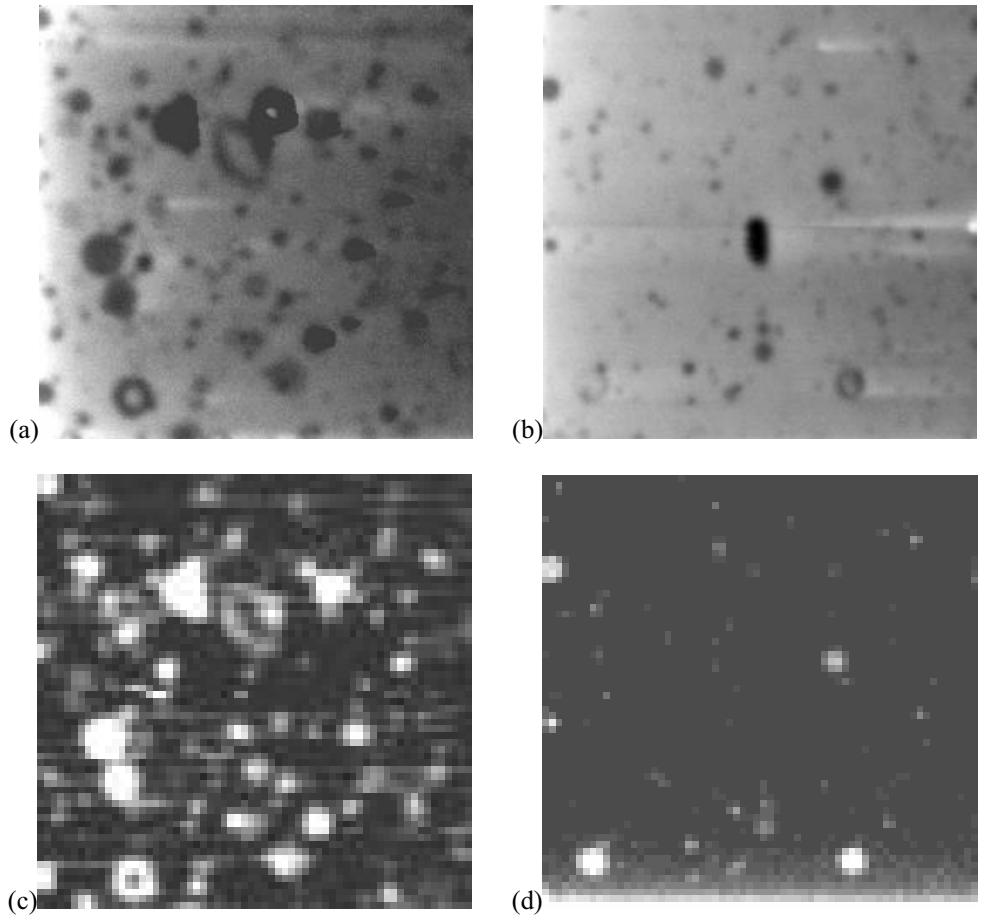

Figure 7: (a) Auger electron microcopy image of 50μm x 50μm of surface exposed without the repeller field,
(b) Auger electron microcopy image of 50μm x 50μm of surface exposed with the repeller field,
(c) Auger electron microscopy image of tin elemental mapping of the same area as (a),
(d) Tin elemental mapping of the same area as (b).

3.2.2. Effect of repeller field for stopping ions

We already reported observations that ions from a water droplet plasma eroded the multilayer mirror surface, and that repeller fields improved the mirror reflectivity lifetime[10]. The main mechanism of erosion in these early experiments resulted from erosion due to oxygen ions. The sputtering effect of the oxygen ions was lowered in the presence of the repeller field. This is possibly a consequence of the energy of the oxygen ions being lowered by the field. We verified the effect of repeller field on ions by placing the ion probe, instead of witness plates, behind the field. The schematic is shown in Fig. 8. A typical IP signal is shown in Fig. 9 for the case when the laser energy was 340mJ.

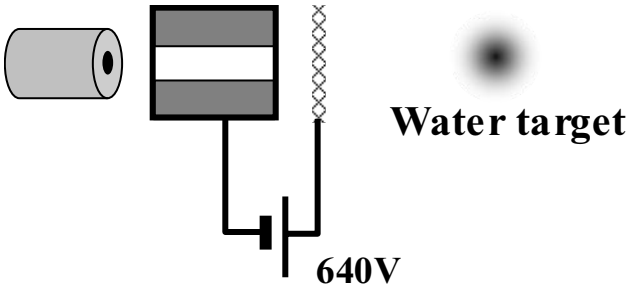

Figure 8: Measurement of ion signal with repeller field.

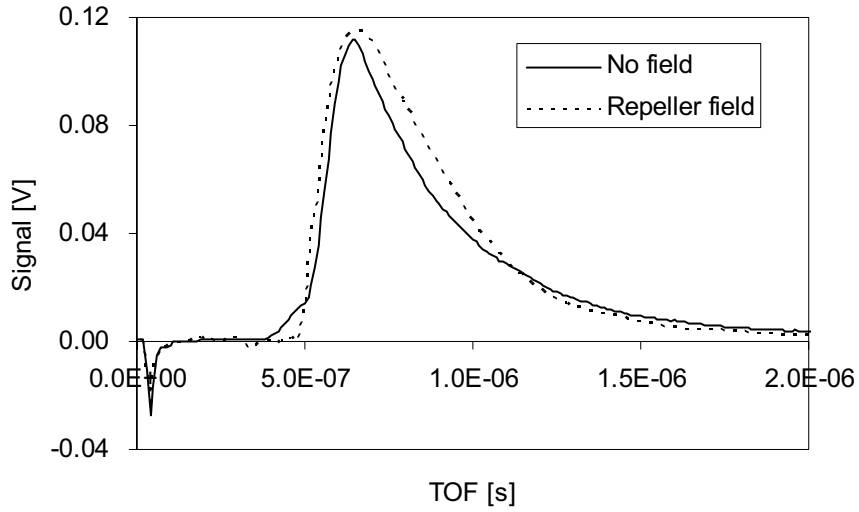

Figure 9: Ion probe signal with / without repeller field.

The signal was averaged over 8 shots in each configuration. Looking at the rise in the ion probe signal, just before 0.5μs, the signature of the fastest ions appears as a step in the signal when no field is applied. This step, however, is not seen in the signal with the repeller field. From the ion spectral measurements, these are hydrogen ions. The hydrogen ions are stopped or slowed down so that the hydrogen ions reach the ion probe at the same time as oxygen ions do. In the latter case, we cannot resolve the hydrogen signal separately from oxygen ion signals. It is clear that the energy of hydrogen ions is lowered. However, it is not seen in the ion probe signal that oxygen ions are slowed down, but the energy of oxygen ions is expected to be lowered. Therefore the ion spectral measurements with the repeller field are necessary to verify the effectiveness of the repeller field for stopping ions.

4. CONCLUSION

This study shows details of the debris from the mass-limited tin based droplet target. Results of ion energy measurements using the Ion Probe and the Ion spectrometer agreed consistently with each other. The repeller field inhibits tin particle depositions as well as fast ions. More methods for measuring ions and for inhibiting ion/particle are necessary in the near future.

ACKNOWLEDGMENTS

The authors wish to acknowledge the technical assistance of colleagues with LPL at the School of Optics/CREOL, particularly Dr G Shimkaveg, Robert Bernath (CREOL) and the assistance at AMPAC/Material Characterization Facility, particularly Kirk Scammon.

REFERENCES

1. Y. Watanabe, “Source requirements,” presentation at ISMT EUV source workshop, Feb. 22, 2004.
2. This work was done under contract for JMar Research Corp, resulting in patents being filed at that time.
3. C-S. Koay, M. C. Richardson et al., "High conversion efficiency tin material laser plasma source for EUVL," SPIE, volume 5037, pages 801-806, 2003.
4. B. Fay et al., “Modular Laser produce Plasma Source for EUV Lithography,” presentation at ISMT EUV source workshop, Sep. 29, 2003.
5. J. Pankert, “Philips’ EUV lamp: Status and Roadmap,” presentation at ISMT EUV source workshop, Sep. 29, 2003.
6. W. T. Silfvast, M. C. Richardson et al., "Laser-Produced Plasmas for Soft X-ray Projection Lithography," Journal of Vacuum Science and Technology B, volume 10, number 6, pages 3126-3133, November 1992.
7. F. Jin, M. C. Richardson et al., "Mass-limited laser plasma cryogenic target for 13 nm point x-ray sources for lithography," Proceedings of SPIE, volume 2015, pages 151-159, 1993.
8. M. C. Richardson et al., "A Debris-Free Laser-Plasma EUV Source Using Ice Droplets," Proceedings of SPIE, volume 3157, pages 306-309, July 1997.
9. K. Takenoshita, M. C. Richardson et al., "The repeller field debris mitigation approach for EUV sources," Emerging Lithographic Technologies VII, SPIE, volume 5037, pages 792-800, 2003.
10. G. Schriever, M. C. Richardson, E. Turcu, "The droplet laser plasma source for EUV lithography," Proceedings of CLEO, pages 393-394, 7-12 May 2000.
11. M. Richardson and G. Schriever, US Patent 6,377,651, (2002)
12. F. Bijkerk et al., “A high-power, low-contamination laser plasma source for Extreme UV lithography,” Microelectronic Engineering, Volume 27, Issues 1-4, February 1995, Pages 299-301
13. H. Yashiro et al., “Study of ultra-fast ion shutter employing a laser-produced plasma,” Emerging Lithographic Technologies VII, SPIE, volume 5037, pages 759-766, 2003.
14. B. Thestrup et al., “A comparison of the laser plume from Cu and YBCO studied with ion probes,” Applied Surface 208-209 (2003), 33-38.
15. L. Torrisi et al., “Ion and neutral emission from pulsed laser irradiation of metals,” Nuclear Instruments and Methods in Physics Research B 184 (2001) 327-336.
16. S S Chowdhury et al., “Ion energy analyzer for laser-produced plasma,” 1980 J. Phys. E: Sci. Instrum. 13 1099-1105